Frontiers of Information Technology & Electronic Engineering
www.jzus.zju.edu.cn; engineering.cae.cn; www.springerlink.com
ISSN 2095-9184 (print); ISSN 2095-9230 (online)
E-mail: jzus@zju.edu.cn

Supplementary materials for

Yuanyuan LI, Xiaoqing YOU, Jianquan LU, Jungang LOU, 2023. A joint image compression and encryption scheme based on a novel coupled map lattice system and DNA operations. *Front Inform Technol Electron Eng*, 24(6):813-827. https://doi.org/10.1631/FITEE.2200645

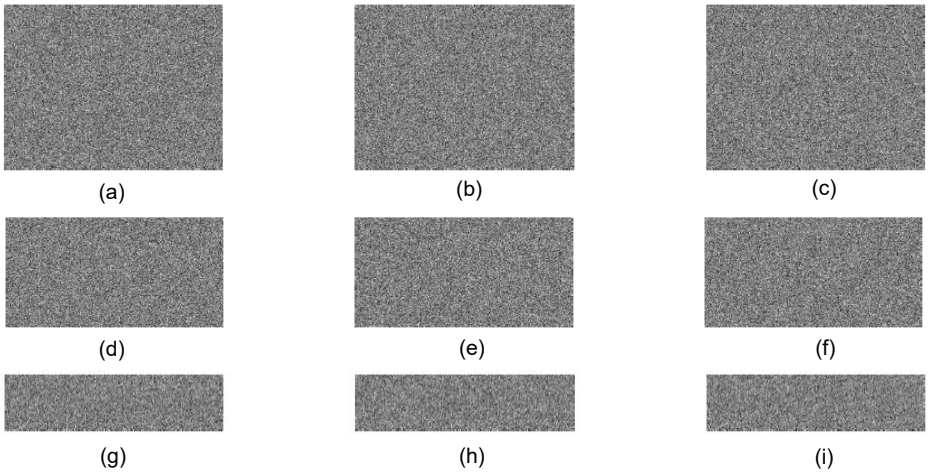

Fig. S1 Cipher images under different compression ratios (CRs)
(a) CR=0.75, Lena; (b) CR=0.75, Peppers; (c) CR=0.75, Baboon; (d) CR=0.50, Lena; (e) CR=0.50, Peppers; (f) CR=0.50, Baboon; (g) CR=0.25, Lena; (h) CR=0.25, Peppers; (i) CR=0.25, Baboon

Table S1 Differences between cipher images produced by slightly different keys

Figure	Encryption keys	Difference ratio from Fig. 5b (%)
Fig. S5a	$x_1' = x(1) + 10^{-10}, x_2, ..., x(10)$	99.5956
Fig. S5b	$x_2' = x(1), x_2 + 10^{-10}, ..., x(10)$	99.6048
Fig. S5c	$x_5' = x(1), ..., x(5) + 10^{-10}, ..., x(10)$	99.6140
Fig. S5d	$x_9' = x(1), x_2, ..., x(9) + 10^{-10}, x(10)$	99.6361
Fig. S5e	$x_{10}' = x(1), x_2, ..., x(9), x(10) + 10^{-10}$	99.5964

Table S2 r_{xy} of adjacent pixels in the plain and cipher images

Image		Correlation coefficient		
		Horizontal	Vertical	Diagonal
Lena	Plain image	0.9692	0.9842	0.9640
	Cipher image	−0.0010	−0.0014	−0.0029
Peppers	Plain image	0.9733	0.9763	0.9650
	Cipher image	0.0056	0.0011	0.0004
Baboon	Plain image	0.8622	0.7471	0.7155
	Cipher image	0.0026	0.0030	−0.0017

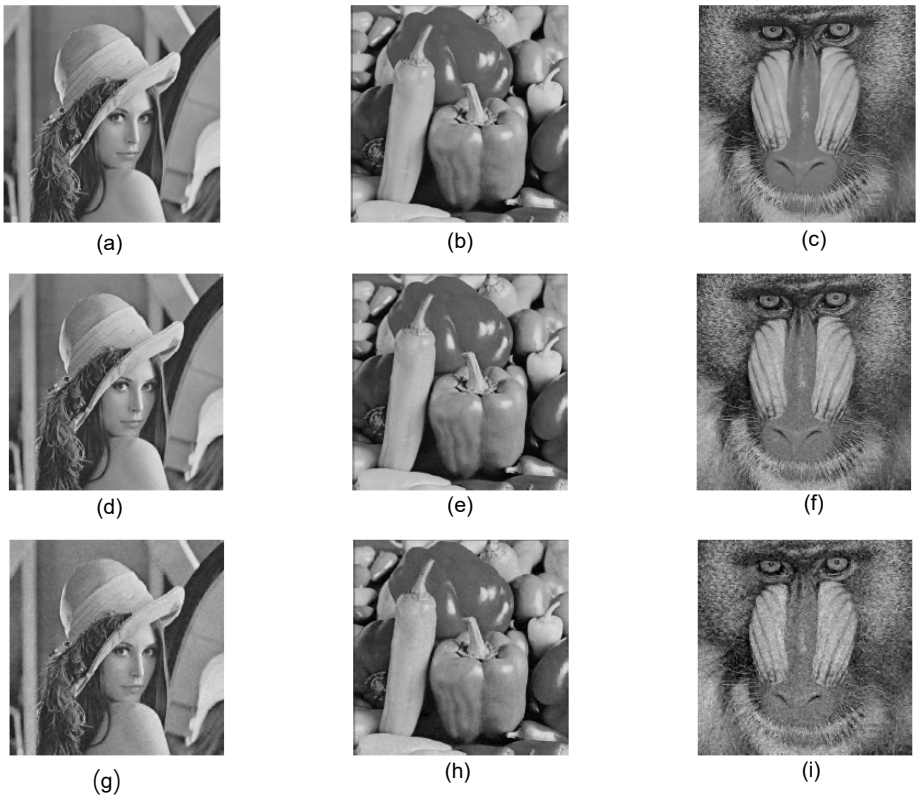

Fig. S2 Decrypted images under different CRs

(a) CR=0.75, PSNR=34.4300 dB; (b) CR=0.75, PSNR=34.1785 dB; (c) CR=0.75, PSNR=34.0133 dB; (d) CR=0.50, PSNR=33.4462 dB; (e) CR=0.50, PSNR=33.7960 dB; (f) CR=0.50, PSNR=32.1523 dB; (g) CR=0.25, PSNR=28.1009 dB; (h) CR=0.25, PSNR=30.9583 dB; (i) CR=0.25, PSNR=28.0046 dB

Table S3 Information entropies of plain and cipher images

Image	Information entropy	
	Plain image	Cipher image
Lena	7.4474	7.9986
Peppers	7.3967	7.9987
Baboon	7.3814	7.9987

Table S4 Information entropy comparison among different methods

Algorithm	Ours	Gan et al. (2020)	Li XH et al. (2022)	Li LX et al. (2019)	Chai et al. (2020a)
Information entropy	7.9986	7.9986	7.9976	7.9857	4.1120

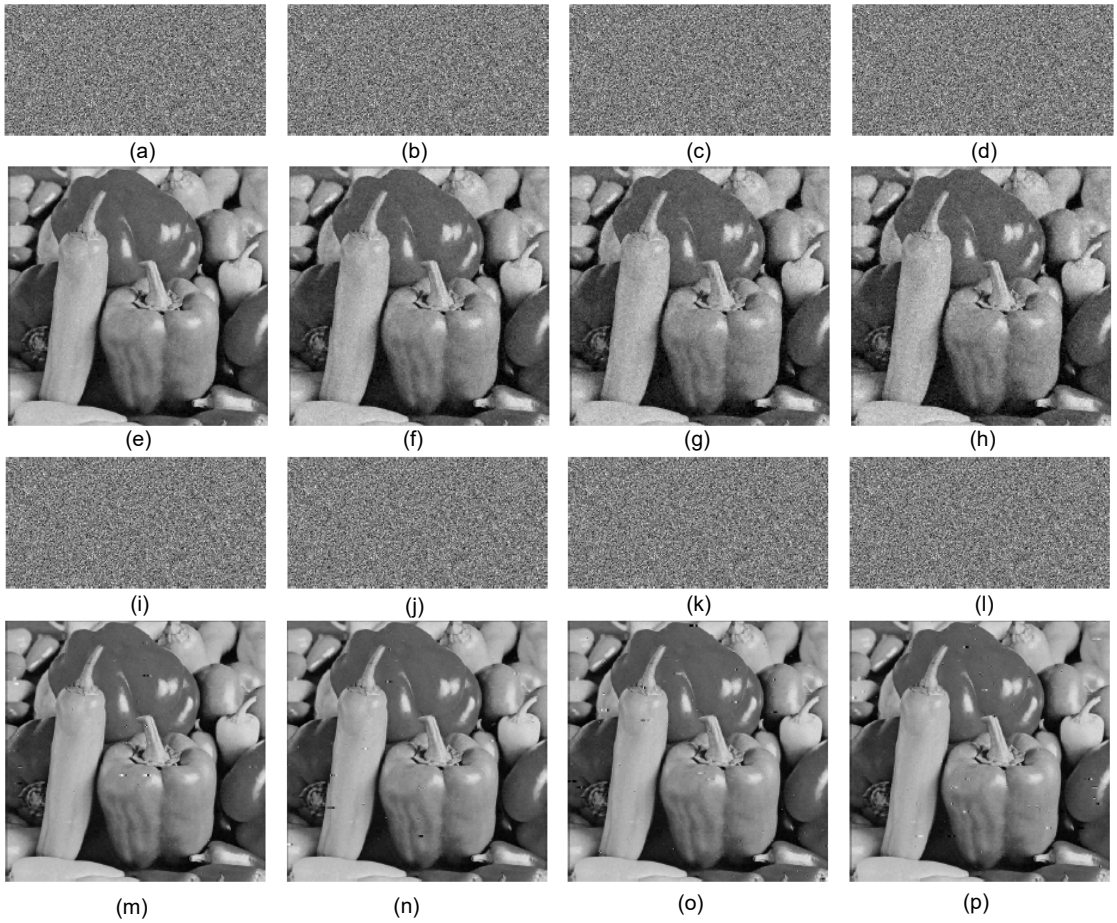

Fig. S3 Cipher and decrypted images under different intensities of Gaussian noise (GN) and salt pepper noise (SPN) attacks
(a) GN with an intensity of 0.000 01; (b) GN with an intensity of 0.000 03; (c) GN with an intensity of 0.000 05; (d) GN with an intensity of 0.000 07; (e) decrypted image of (a); (f) decrypted image of (b); (g) decrypted image of (c); (h) decrypted image of (d); (i) SPN with an intensity of 0.000 01; (j) SPN with an intensity of 0.000 03; (k) SPN with an intensity of 0.000 05; (l) SPN with an intensity of 0.000 07; (m) decrypted image of (i); (n) decrypted image of (j); (o) decrypted image of (k); (p) decrypted image of (l)

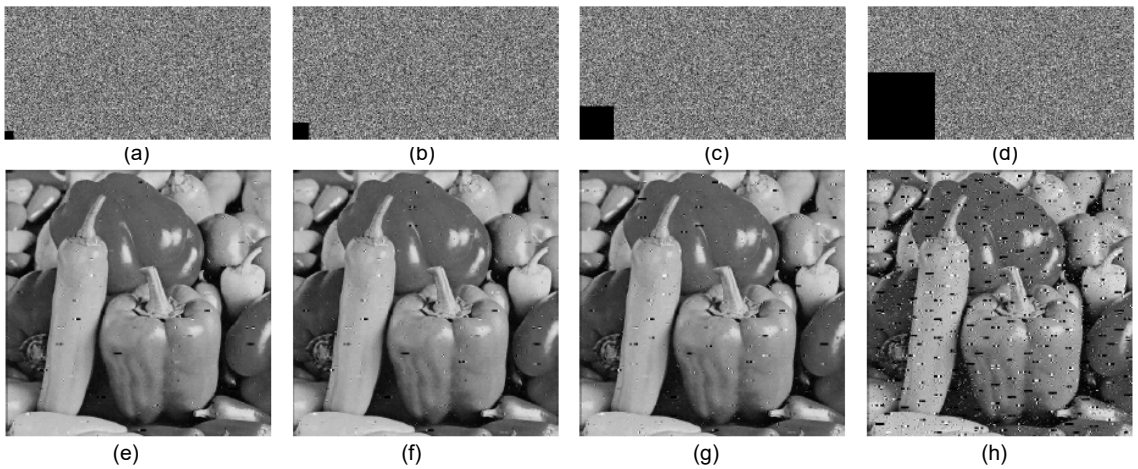

Fig. S4 Cipher and decrypted images under different degrees of data loss attacks
(a) 16×16 data loss; (b) 32×32 data loss; (c) 64×64 data loss; (d) 128×128 data loss; (e) decrypted image of (a); (f) decrypted image of (b); (g) decrypted image of (c); (h) decrypted image of (d)

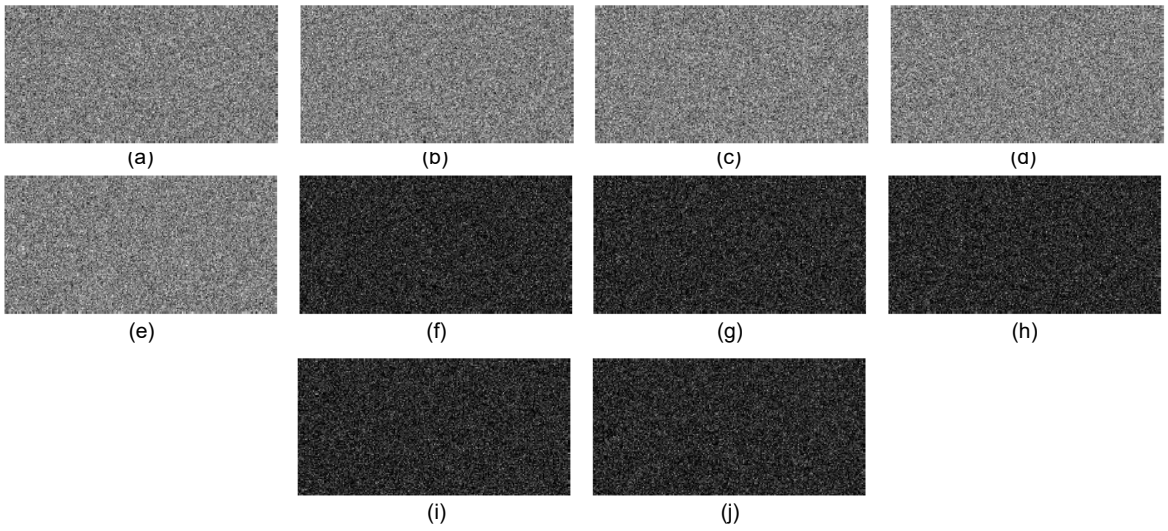

Fig. S5 Key sensitivity test in the first case

(a) cipher image with x_1'; (b) cipher image with x_2'; (c) cipher image with x_5'; (d) cipher image with x_9'; (e) cipher image with x_{10}'; (f) subtraction of (a); (g) subtraction of (b); (h) subtraction of (c); (i) subtraction of (d); (j) subtraction of (e)

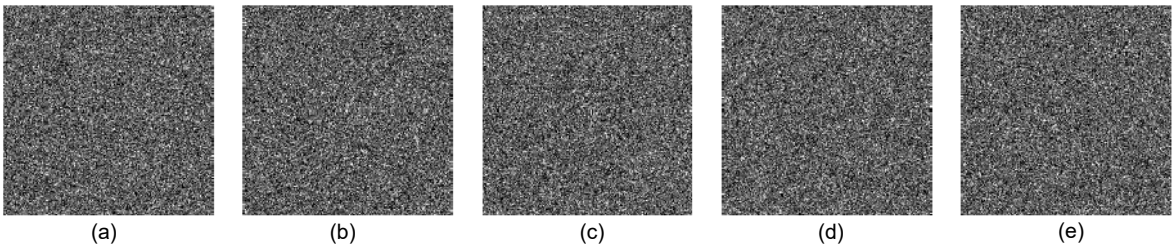

Fig. S6 Key sensitivity test in the second case

(a) decrypted image with x_1'; (b) decrypted image with x_2'; (c) decrypted image with x_5'; (d) decrypted image with x_9'; (e) decrypted image with x_{10}'

Table S5 Differential attack resistance of the proposed scheme

Image	Pixel modification	NPCR	UACI
Lena	$P_{(1, 1)}$=162→163	0.9962	0.3352
	$P_{(251, 266)}$=153→154	0.9960	0.3357
	$P_{(512, 512)}$=108→107	0.9960	0.3348
Peppers	$P_{(1, 1)}$=30→29	0.9960	0.3350
	$P_{(199, 437)}$=188→187	0.9961	0.3349
	$P_{(512, 512)}$=196→197	0.9962	0.3353
Baboon	$P_{(1, 1)}$=128→129	0.9961	0.3348
	$P_{(343, 93)}$=4→5	0.9961	0.3347
	$P_{(512, 512)}$=55→54	0.9959	0.3342

NPCR: number of pixel change rate; UACI: unified averaged changed intensity

Table S6 Encryption time comparison among different methods

Algorithm	Ours	Chai et al. (2020a)	Li LX et al. (2019)	Chai et al. (2020b)	Gan et al. (2020)	Li XH et al. (2022)
Time (s)	1.9352	0.52	1.8381	2.53	>5	>14.92

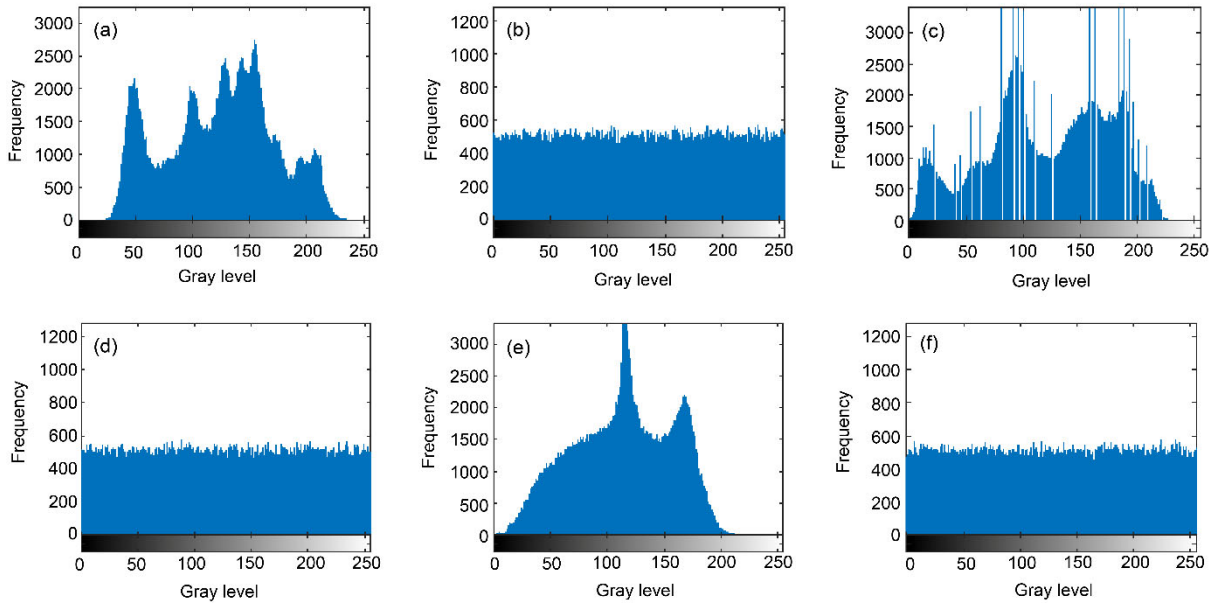

Fig. S7 Histogram information for plain and cipher images

(a) histogram of plain image Lena; (b) histogram of cipher image Lena; (c) histogram of plain image Peppers; (d) histogram of cipher image Peppers; (e) histogram of plain image Baboon; (f) histogram of cipher image Baboon

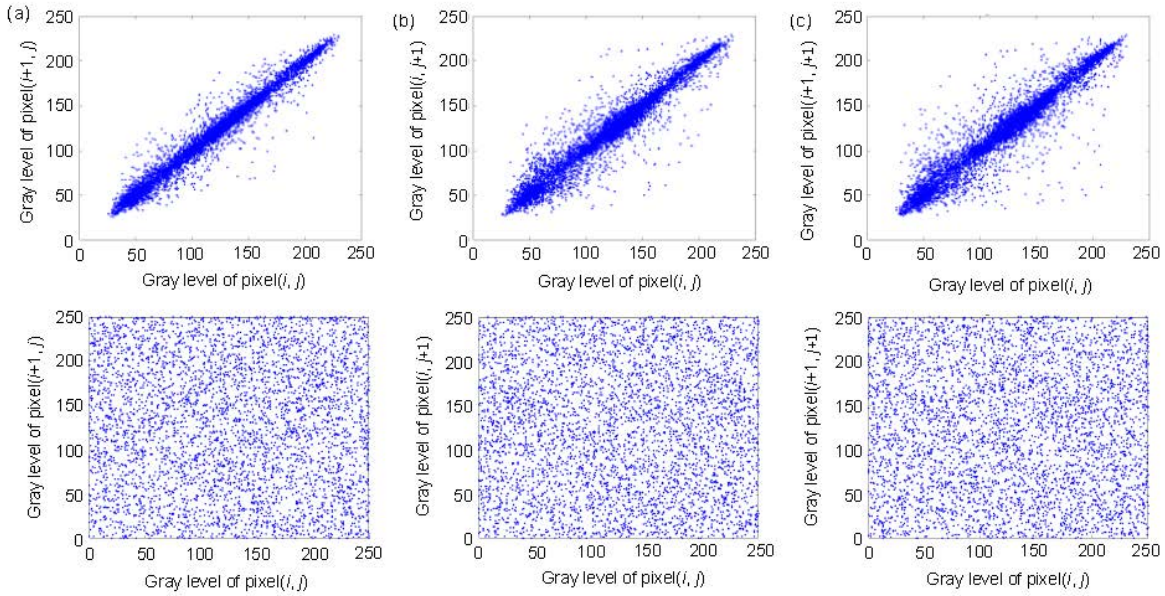

Fig. S8 Correlation distributions of image Lena and its cipher image

(a) horizontal direction; (b) vertical direction; (c) diagonal direction

Table S7 Reconstruction time comparison among different semi-tensor product measurements

Size	256×512 (traditional CS)	128×256	64×128	32×64
Time (s)	18.4771	12.7513	5.9774	4.8479

CS: compressive sensing

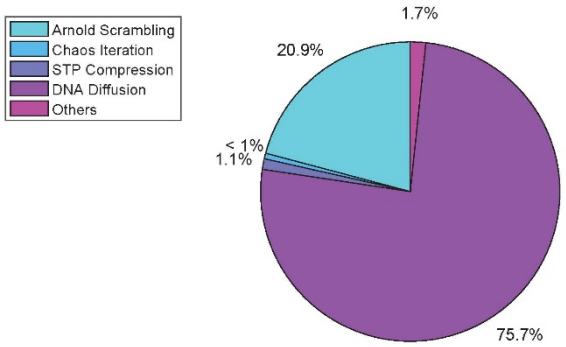

Fig. S9 Time proportion of different encryption phases

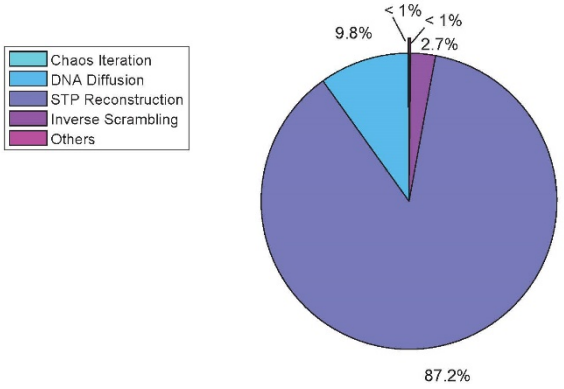

Fig. S10 Time proportion of different decryption phases

References

Chai XL, Fu XL, Gan ZH, et al., 2020a. An efficient chaosbased image compression and encryption scheme using block compressive sensing and elementary cellular automata. *Neur Comput Appl*, 32(9):4961-4988. https://doi.org/10.1007/s00521-018-3913-3

Chai XL, Wu HY, Gan ZH, et al., 2020b. An efficient visually meaningful image compression and encryption scheme based on compressive sensing and dynamic LSB embedding. *Opt Lasers Eng*, 124:105837. https://doi.org/10.1016/j.optlaseng.2019.105837

Gan ZH, Chai XL, Zhang JT, et al., 2020. An effective image compression-encryption scheme based on compressive sensing (CS) and game of life (GOL). *Neur Comput Appl*, 32(17):14113-14141. https://doi.org/10.1007/s00521-020-04808-8

Li LX, Liu LF, Peng HP, et al., 2019. Flexible and secure data transmission system based on semitensor compressive sensing in wireless body area networks. *IEEE Internet Things J*, 6:3212-3227. https://doi.org/10.1109/JIOT.2018.2881129

Li XH, Zhou LL, Tan F, 2022. An image encryption scheme based on finite-time cluster synchronization of two-layer complex dynamic networks. *Soft Comput*, 26(2):511-525. https://doi.org/10.1007/s00500-021-06500-y